

# A Polyelectrolyte Handle for Single-Molecule Force Spectroscopy

*Junpeng Wang<sup>1</sup>, Tatiana B. Kouznetsova<sup>1</sup>, Jianshe Xia<sup>2</sup>, Felipe Jiménez Ángeles<sup>2</sup>, Monica Olvera de la Cruz<sup>2,\*</sup>, and Stephen L. Craig<sup>1,\*</sup>*

<sup>1</sup>Department of Chemistry, Duke University, Durham, North Carolina, 27708, USA, <sup>2</sup>Department of Materials Science and Engineering, Northwestern University, Evanston, Illinois, 60208, USA

**Accepted for publication at *J. Polym. Sci.***

**Abstract:** Single-molecule force spectroscopy is a powerful tool for the quantitative investigation of the biophysics, polymer physics and mechanochemistry of individual polymer strands. One limitation of this technique is that the attachment between the tip of the atomic force microscope and the covalent or noncovalent analyte in a given pull is typically not strong enough to sustain the force at which the event of interest occurs, which makes the experiments time-consuming and inhibits throughput. Here we report a polyelectrolyte handle for single-molecule force spectroscopy that offers a combination of high (several hundred pN) attachment forces, good (~4%) success in obtaining a high-force (>200 pN) attachment, a non-fouling detachment process that allows for repetition, and specific attachment locations along the polymer analyte.

## Introduction

Since its invention in the 1980s,<sup>1</sup> the precision of the atomic force microscope (AFM) in force measurement and surface/tip displacement have enabled AFM-based single-molecule force spectroscopy (SMFS) to become a versatile technique for probing inter- and intramolecular interactions,<sup>2-5</sup> exploring the dynamic conformations of biomolecules,<sup>6-10</sup> and measuring single chain mechanics.<sup>8,11-14</sup> In recent years, it has also been applied to the field of covalent mechanochemistry,<sup>15-17</sup> where it has provided substantial insights.<sup>18-28</sup>

An ideal SMFS experiment would meet the following criteria: 1) the analyte would attach quickly to the AFM tip as the tip approaches the substrate; 2) the site of analyte attachment to the AFM tip would be known in advance; 3) the attachment between analyte and tip would be strong enough to sustain the force required to activate the transformation of interest; 4) rupture of the attachment between AFM tip and the analyte would occur cleanly so that the experiment can be repeated multiple times with a single tip. Criteria 3 and 4 require the attachment between the tip and the polymer to be strong relative to the process of interest, but weak relative to bond scission in the analyte as well as to detachment of the polymer from the surface.

When SMFS experiments rely on “fishing” for non-specific attachments, the force between the AFM tip and the polymer in a given pull is usually too weak to sustain the force required to activate the analyte; thus it often takes hundreds or even thousands of “casts” to obtain a successful pull. This challenge is particularly acute for covalent mechanochemistry, which requires forces on the level of 100s of pN or even nN in order to activate covalent mechanophores on the SMFS time scale.<sup>29</sup> The combination of main-chain epoxidized polymers and oxidized tips has proven useful in some systems,<sup>23-24,30</sup> but many potential analytes either do not possess a main-chain alkene for

epoxidation or are vulnerable to unwanted side reactions. We therefore sought complementary strategies that might meet the criteria described above.

Our design is shown in Figure 1. To one end of a polymer analyte of interest a polyelectrolyte block is appended, which we hypothesized might form a rapid attachment to an oppositely charged AFM tip. Because electrostatic interactions are relatively long-ranged, the effective capture radius for attachment upon approach might increase, although we note that larger capture radius has been correlated with off-angle pulling that might require active control to mitigate.<sup>31-33</sup> Furthermore, the magnitude of the attachment force would depend on the number of charges and other experimental conditions, such as counterions and solvents. This combination of potential properties led us to investigate polyelectrolyte handles as a tool for SMFS.

To investigate the potential utility of this strategy, we chose the widely used polyelectrolyte poly(2-dimethylaminoethyl methacrylate) (PDMAEMA).<sup>34</sup> PDMAEMA has been synthesized using different controlled/living radical polymerization methods, including reversible addition fragmentation chain transfer polymerization (RAFT),<sup>35</sup> stable free radical polymerization (SFRP),<sup>36</sup> and atom transfer radical polymerization (ATRP).<sup>37-39</sup> RAFT is advantageous over other polymerization methods in that the corresponding polymer is produced with a dithioester end

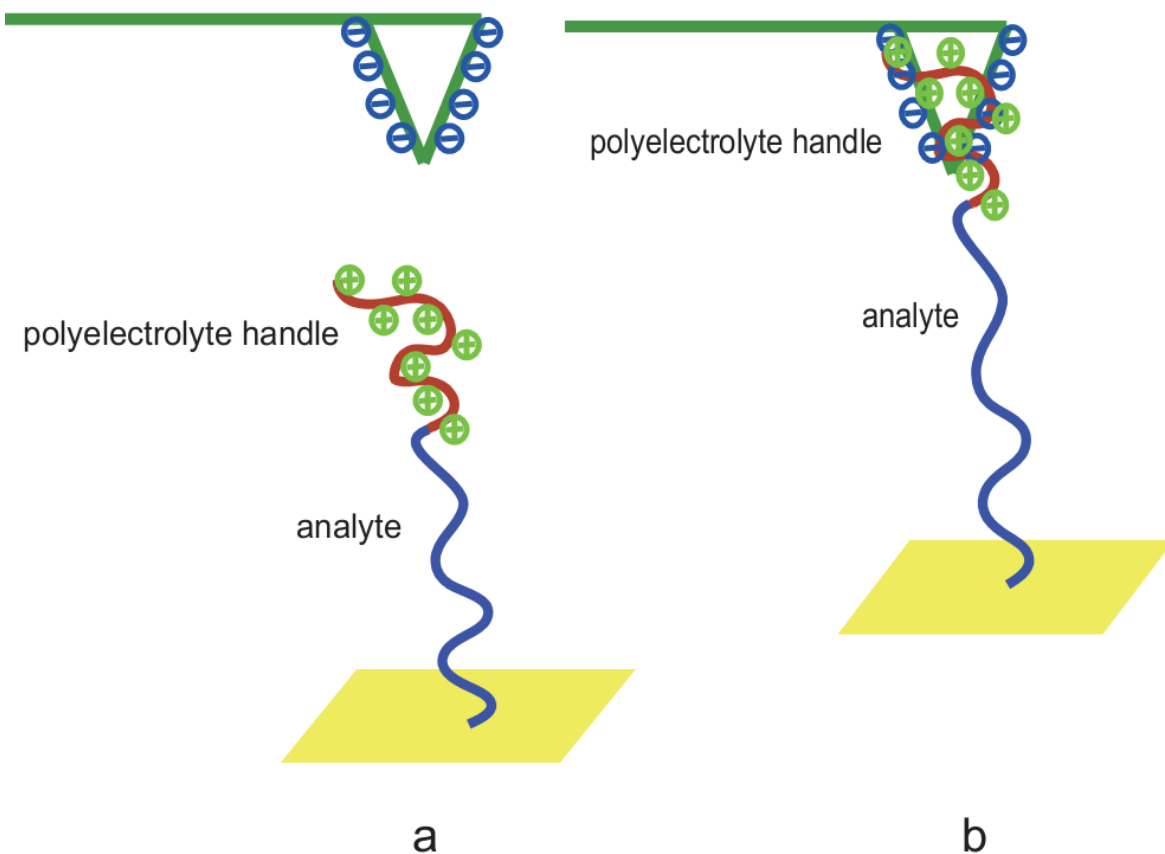


**Figure 1.** **(a)** The polymer analyte to be studied (blue line) was incorporated to a polyelectrolyte handle which contains positive charges (red line). The AFM tip was modified with a SAM of negative charge. **(b)** When the surface is brought into proximity with the tip, the polyelectrolyte handle bonds to the tip via an electrostatic interaction.

group, which can then be grafted to the gold surface directly.<sup>40</sup> This saves a step of end-group functionalization for attaching the polymer to the surface. To test the performance of the handle and to identify conditions that satisfy the criteria discussed above, a series of block copolymers,

each containing a polyelectrolyte handle and a neutral analyte region, were made via RAFT. The polymers were grafted to a gold surface, and the resulting SMFS behavior of the system was studied.

## Materials and methods

2-(dimethylamino) ethyl methacrylate (DMAEMA) and 2-ethoxyethyl methacrylate (EOEMA) were purchased from Sigma Aldrich and purified through a basic aluminum oxide column to remove the inhibitor before being used for polymerization. 4-Cyanopentanoic acid dithiobenzoate (CPADB), 4,4'-azobis(4-cyanovaleric acid) (V501), methyl iodide, tetrahydrofuran (THF, inhibitor free), triethylamine, methyl benzoate, diphenyl ether, 11-mecaptoundecanoic acid, 1-undecanethiol, silver hexafluorophosphate, mesitylene and 1-butanol were also purchased from Sigma Aldrich and used as received. Dichloromethane, hexane, acetonitrile, acetone, ethanol and dimethylformamide (DMF) were purchased from VWR and used as received. Each Au coated substrate was obtained by sputtering 10 nm of Ti and then 150 nm of Au on a Si (111) wafer. Polymers were characterized using <sup>1</sup>H-NMR and gel permeation chromatography (GPC). The GPC experiments were performed on an in-line two column system (Agilent Technology PL Gel, 10<sup>3</sup> and 10<sup>4</sup> Å) using THF with 3% triethylamine as the eluent. Molecular weights were calculated using a Wyatt Dawn EOS multi-angle light scattering (MALS) detector and a Wyatt Optilab DSP Interferometric Refractometer (RI). The refractive index increment ( $dn/dc$ ) values were determined by online calculation using injections of known concentration and volume. The polymers were grafted to a Au surface and characterized with a variable angle spectroscopic ellipsometer (J.A. Woollam, Inc.), X-ray photoelectron spectroscopy (XPS), and water contact angle goniometer.

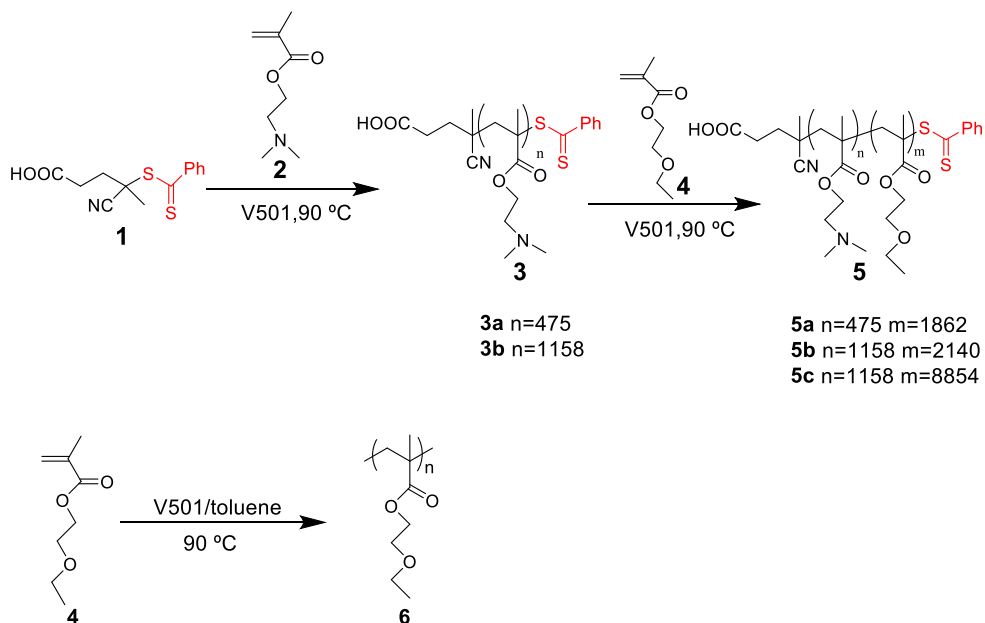
Details of polymer synthesis, characterization and surface modification are described in Supporting Information (SI).

The AFM experiments were conducted in deionized water, DMF, 1-butanol, methyl benzoate, diphenyl ether and mesitylene. All of the experiments were performed at room temperature using a homemade AFM, constructed with a Digital Instruments scanning head mounted on top of a piezoelectric positioner.<sup>41</sup> Standard NPG probes whose tips were coated with Au on Si<sub>3</sub>N<sub>4</sub> were purchased from Bruker (Camarillo, CA). The cantilevers were V shaped (205  $\mu$ m  $\times$  25  $\mu$ m, nominal tip radius  $\sim$  30 nm, nominal spring constant k  $\sim$  0.06 N/m, frequency  $\sim$  18 kHz). The spring constant of each cantilever was calibrated in air, using the MFP 3D system (Asylum Research Group Inc., Santa Barbara, CA), by applying the thermal noise method, based on the energy equipartition theorem as described previously.<sup>42</sup> The Au coated tips were functionalized with a SAM of carboxylate by immersing in 5 mM EtOH solution of 11-mercaptoundecanoic acid and ionizing in 0.1 M K<sub>2</sub>CO<sub>3</sub> aqueous solution overnight (typically  $\sim$ 16 h). The cantilever was then mounted in a fluid cell and set up with the AFM head. The Au coated substrate with functionalized polymer was placed on the piezoelectric stage of the AFM for measurement. A series of approach/retract cycles were performed, and the data was collected by dSPACE (dSPACE Inc., Wixom, MI) and analyzed using Matlab (The Math Works, Inc., Natick, MA).

## Results

Three different block copolymers **5a**, **5b** and **5c** (Scheme 1) were synthesized via RAFT. **5a** and **5b** have different DMAEMA lengths and similar EOEMA lengths, whereas **5b** and **5c** have the same length of DMAEMA and different lengths of EOEMA.

**Scheme 1. Synthesis of block copolymers and control polymer.**



Au coated substrates were placed in 1 mg/mL dichloromethane solutions of polymers **5a-c** and **6** (Scheme 1) for 24 h and then rinsed with dichloromethane extensively to remove the physically absorbed polymers. Ellipsometry (Table 1) shows that less of polymer **6** is attached to Au surface compared to polymers **5a-c**, which supports that polymers **5a-c** are attached to Au surface via the Au-S bonds (Figure 2).

**Table 1. Ellipsometric thicknesses, grafting densities and static water contact angles of Au surface after polymers grafted to the surface.**

Au surface with polymer	ellipsometric thickness (nm)	grafting density (nm <sup>-2</sup> )	water contact angle (°)		
			Neutral	+ MeI	+ AgPF <sub>6</sub>
<b>5a</b>	10.3	$1.64 \times 10^{-2}$	50	56	33
<b>5b</b>	12.0	$1.38 \times 10^{-2}$	48	57	34

<b>5c</b>	13.9	$5.4 \times 10^{-3}$	49	59	36
<b>6</b>	0.3	$6.6 \times 10^{-5}$	-	-	-

The grafting density ( $\sigma$ ) of the surface-anchored polymers was calculated from the ellipsometric thickness using the equation:  $\sigma = hQN_A/M_n$ ,<sup>43</sup> where  $h$  is the ellipsometric thickness,  $N_A$  is Avogadro's number,  $M_n$  is the number average molecular weight of the polymer and  $Q$  is the density of the polymer, approximately 1 g/cm<sup>3</sup>.<sup>44</sup> The grafting density results are shown in Table 1.

After grafting polymers **5a-c** to the Au surface, methyl iodide was used to ionize the polymer. Table 1 shows that the water contact angle slightly increases after the polymer is treated with methyl iodide. The increased hydrophobicity might be caused by the disruption of hydrogen bonding between the amine and water after quaternization.<sup>45</sup>

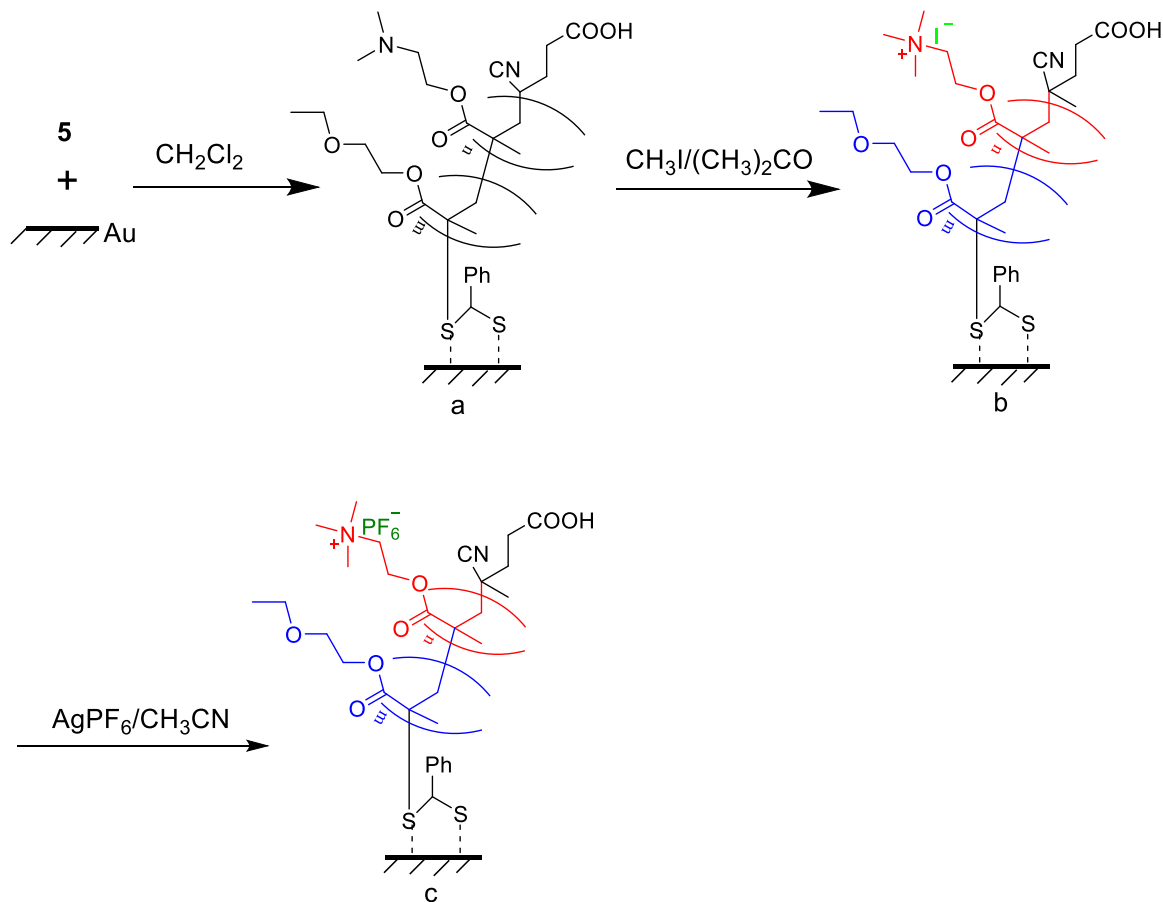


**Figure 2.** Surface treatments. a) Grafting polymer **5** to Au surface. b) Ionizing the polymer by reacting with methyl iodide. c) Counterion exchange by reacting with  $\text{AgPF}_6$ .

Upon treating the ionized polymer surface with  $\text{AgPF}_6$ , a dramatic decrease in water contact angle (Table 1) indicates ion exchange from  $\text{I}^-$  to  $\text{PF}_6^-$ . This trend is consistent with a previous report on the influence of counterions on the wettability of polymer brush surfaces.<sup>46</sup> XPS (**Error! Reference source not found.**<sup>S8</sup>) is also consistent with the desired quaternization by methyl iodide and subsequent counterion exchange.

The polymer grafted surface was brought into contact with, and retracted from, the AFM tip, and the approach/retract cycles were repeated multiple times. From the approach/retract cycles, a

series of force curves were obtained. Figure 3 shows a representative example of a force-extension curve with high detachment force that was obtained during the experiments. The force and length at rupture (point of maximum force) were recorded as a function of various experimental parameters.

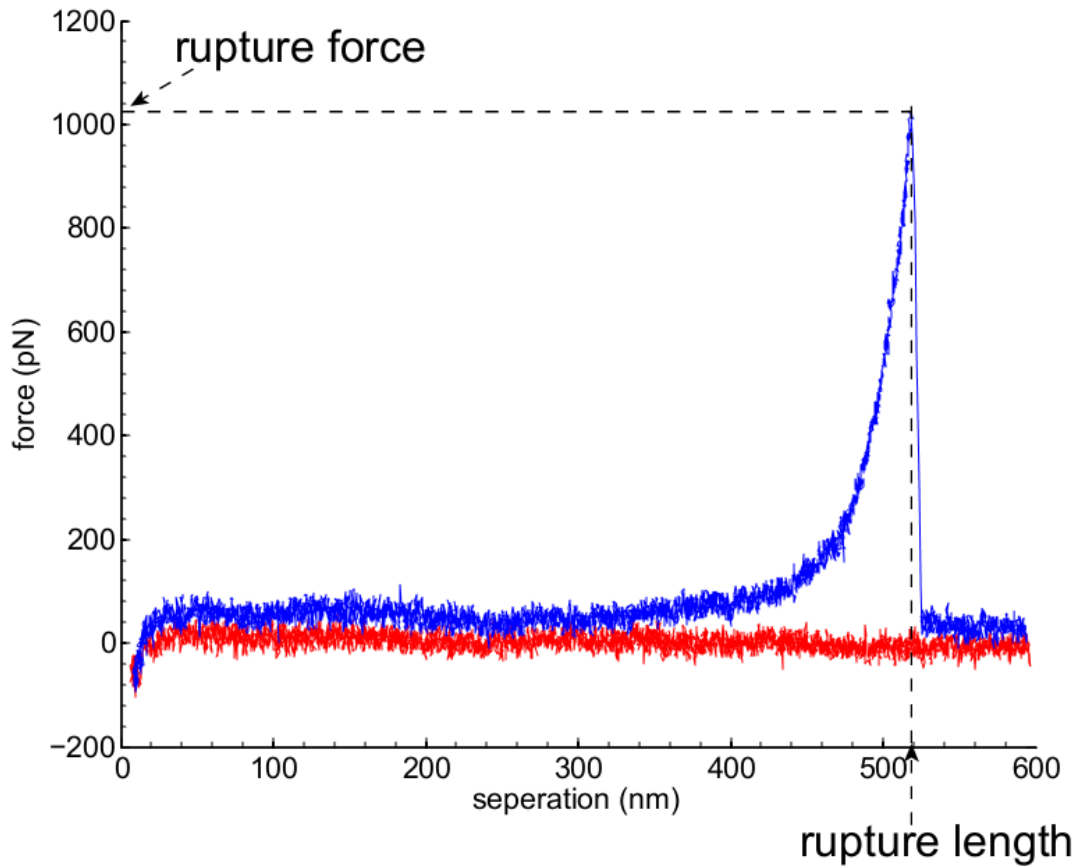


**Figure 3.** A representative force-separation curve persisting to high detachment force obtained in our experiments. After a bridge forms between the AFM tip and the substrate, the polymer is stretched by increasing the distance between tip and substrate. As the separation distance increases, the tensile force on the bridge increases until rupture happened. The force at which rupture occurs is denoted as the rupture force, and the distance denoted as the rupture length.

Grafting density was tuned to identify conditions that are dominated by single chain events. The competing reagent 1-undecanethiol was added to the polymer solution to dilute the density of

grafted polymer on the Au surface. As the concentration of the competing reagent increases, the grafting density decreases (Table 1). For example, as the grafting density of polymer **5b** decreased from  $1.38 \times 10^{-2} \text{ nm}^{-2}$  to  $1.0 \times 10^{-2} \text{ nm}^{-2}$  to  $5.2 \times 10^{-3} \text{ nm}^{-2}$ , the distribution of the rupture force shifts steadily to lower forces. In contrast, when the grafting density decreases from  $5.2 \times 10^{-3} \text{ nm}^{-3}$  to  $2.1 \times 10^{-3} \text{ nm}^{-2}$ , the distribution of the rupture force stays nearly constant (Figure 4), suggesting that  $\sigma = 5.2 \times 10^{-3} \text{ nm}^{-3}$  or less leads to a predominance of single molecule events. That conclusion is supported by overlays of normalized force-extension curves (Figure S9). All experiments reported below were performed at grafting densities of less than  $5.2 \times 10^{-3} \text{ nm}^{-2}$ .

The goal was to use electrostatic interactions to bind to tip, and since the polyelectrolyte is in positive charge, so we expected that a negatively charged tip would generate larger forces. The rupture force distributions obtained for polymer **5a** ( $\text{I}^-$  as counterion) with carboxylate modified

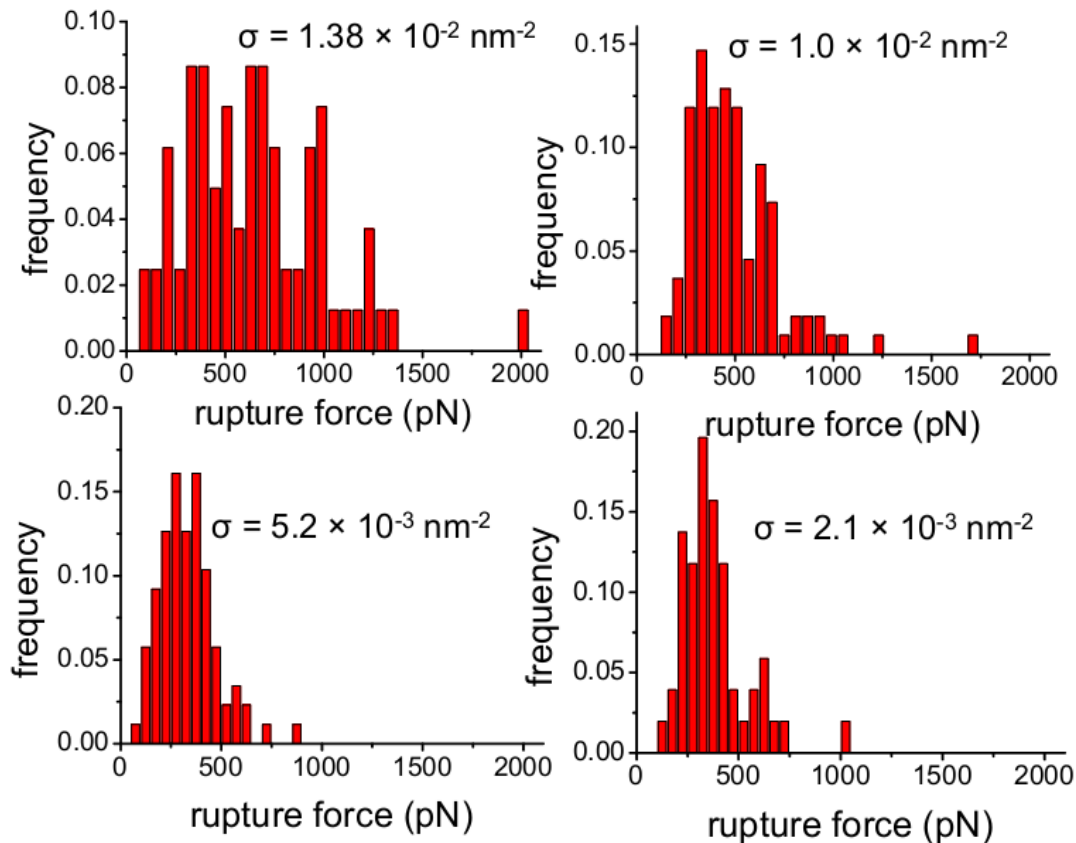


**Figure 4.** Rupture force distributions for different grafting densities of polymer **5b**: (a)  $1.38 \times 10^{-2} \text{ nm}^{-2}$  (b)  $1.0 \times 10^{-2} \text{ nm}^{-2}$  (c)  $5.2 \times 10^{-3} \text{ nm}^{-2}$  (d)  $2.1 \times 10^{-3} \text{ nm}^{-2}$ . The distributions change from (a) to (b) to (c), indicating that (a) and (b) have some multiple-molecule events. (c) and (d) have the same force distribution implying that single-molecule events become predominant in (c) and (d). The force distributions exhibit a peak at  $\sim 250\text{-}300 \text{ pN}$  in all cases, but with more frequent events at higher forces in the systems with higher grafting density.

tip and with bare Au tip were compared in Figure 5. The most probable rupture force obtained with carboxylate modified tip is larger than that obtained with the bare Au tip, indicating that the ionic attachment is stronger than the nonspecific force.

If electrostatic interactions are the major contributor to the polymer-tip interaction, the strength of the attachment should depend on the molecular weight of the polyelectrolyte block. Consistent with this expectation, the force distribution for polymer **5b** ( $\text{I}^-$  as the counterion) is shifted to higher forces than that of polymer **5a** (Figure 6). The same is not true for the analyte region of the polymer. As shown in Figure 7, varying the  $M_w$  of the PEOEMA block grown from the same PDMAEMA block results in effectively identical force distributions. The similarity in the attachment strengths is consistent with a picture in which the attachment is dominated by interactions between the AFM tip and the polyelectrolyte block.

Coarse-grained molecular dynamics simulations are also consistent with this picture. A snapshot of a simulated polymer-tip interaction is shown in Figure 8 (simulation details are provided in Supp. Info.). As seen in Figure 8, the polyelectrolyte handle completely adsorbs to the tip, whereas the analyte does not, so that the extensional behavior is dominated by the analyte and the association/dissociation from the tip is dominated by the handle. Simulations under varying conditions suggest that the adsorption is a reasonably robust aspect of the design that is not particularly sensitive to the analyte/handle specifics, Leonard-Jones interaction potential of the polymer, dielectric constant of the solvent, and the charge density on the AFM tip (see Supporting Information).

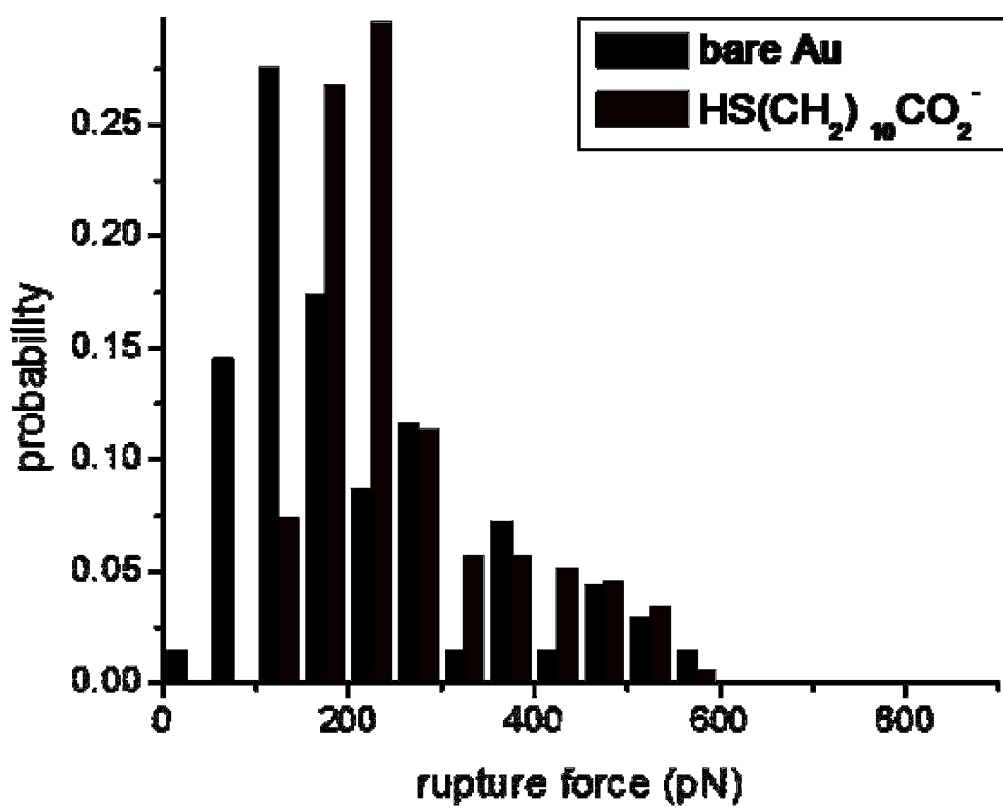


**Figure 5.** The rupture force distributions of polymer **5a** when using bare Au tip (black) and Au tip with a SAM of carboxylate (red). The most probable rupture forces for carboxylate modified tip and bare Au tip are ca. 230 pN and 150 pN, respectively.

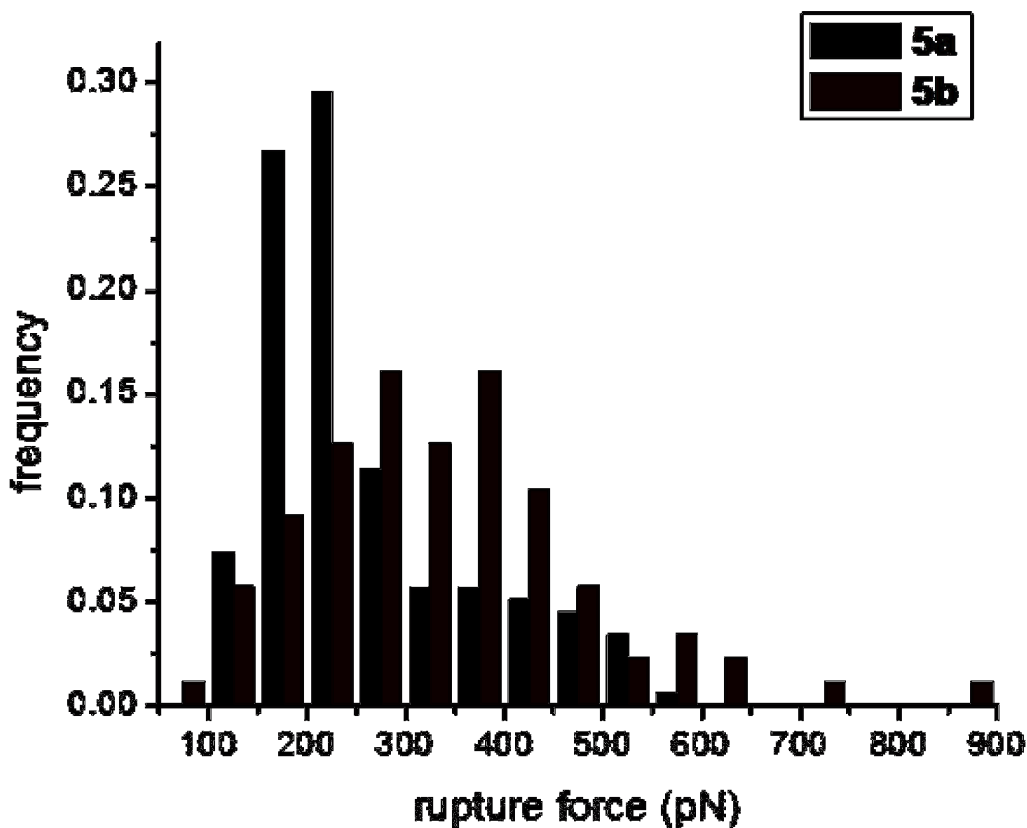


**Figure 6.** The rupture force distributions of polymer **5a** (black) and **5b** (red). The AFM pulling experiments were conducted in methyl benzoate and carboxylate modified tip was used for pulling. The counterion of the polyelectrolyte is iodide for both of the two systems. The most probable rupture force of **5b** is 340 pN while the most probable rupture force of **5a** is 230 pN.

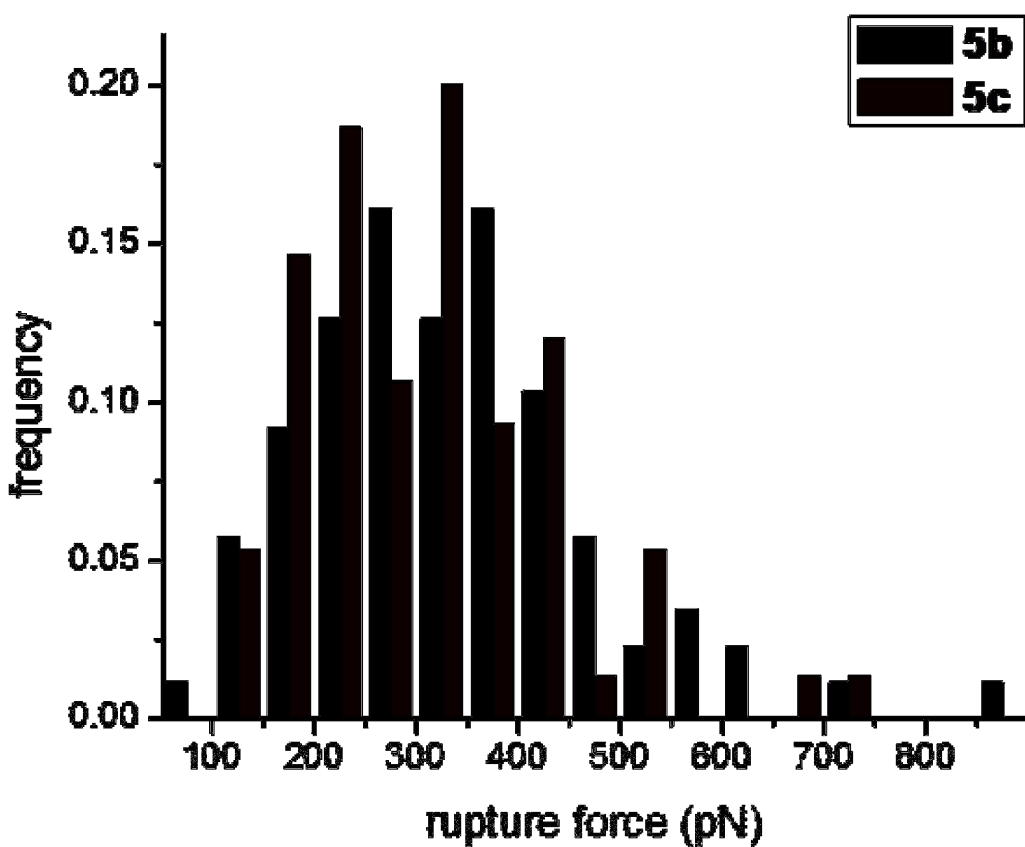


**Figure 7.** The rupture force distributions of polymer **5b** (black) and polymer **5c** (red). The AFM pulling experiments were conducted in methyl benzoate and the carboxylate modified tip was used for pulling. The counterion of the polyelectrolyte was iodide for each system. The force distributions of the two polymers are quite close, with force distributions peaking at ~300 pN in both cases, indicating that the polyelectrolyte part made the main contribution to the strength of the attachment.

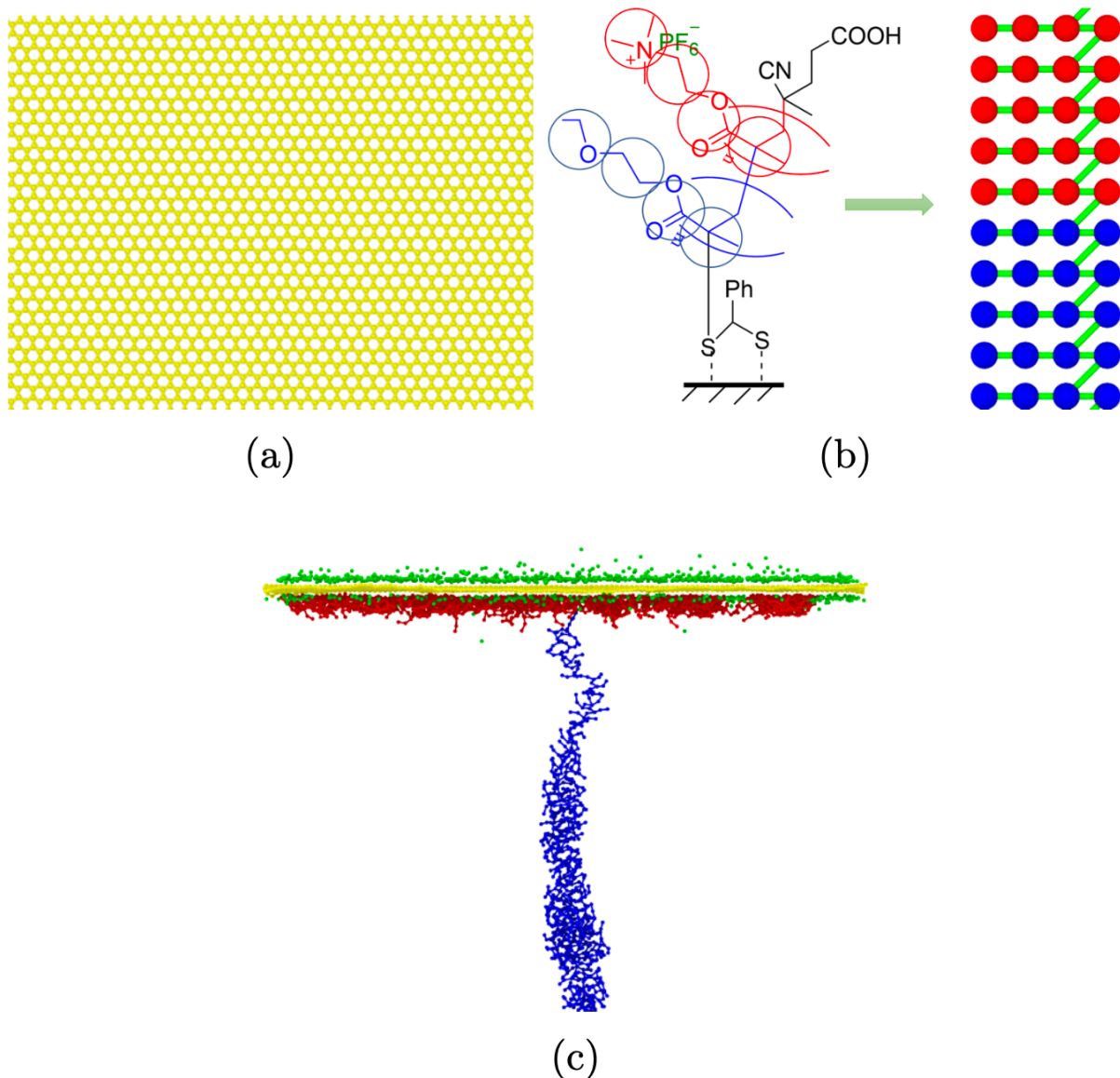


**Figure 8.** Coarse-grained models of the single-molecule force spectroscopy (SMFS) experiments. (a) The squared planar surface of 30 nm per side represents the cross-section of the tip of an atomic force microscope (AFM). (b) Monomers' chemical formula with the coarse-grained scheme for DMAEMA (red) and EOEMA (blue) blocks. The end bead of DMAEMA monomers has a positive charge. (c) Simulation setup representing the SMFS experiment showing the charged block adsorbed on the AFM tip surface while the uncharged block is extended. The green beads are the AFM tip counterions. The polymer counterions are distributed in the simulation box and rarely come near the AFM tip.

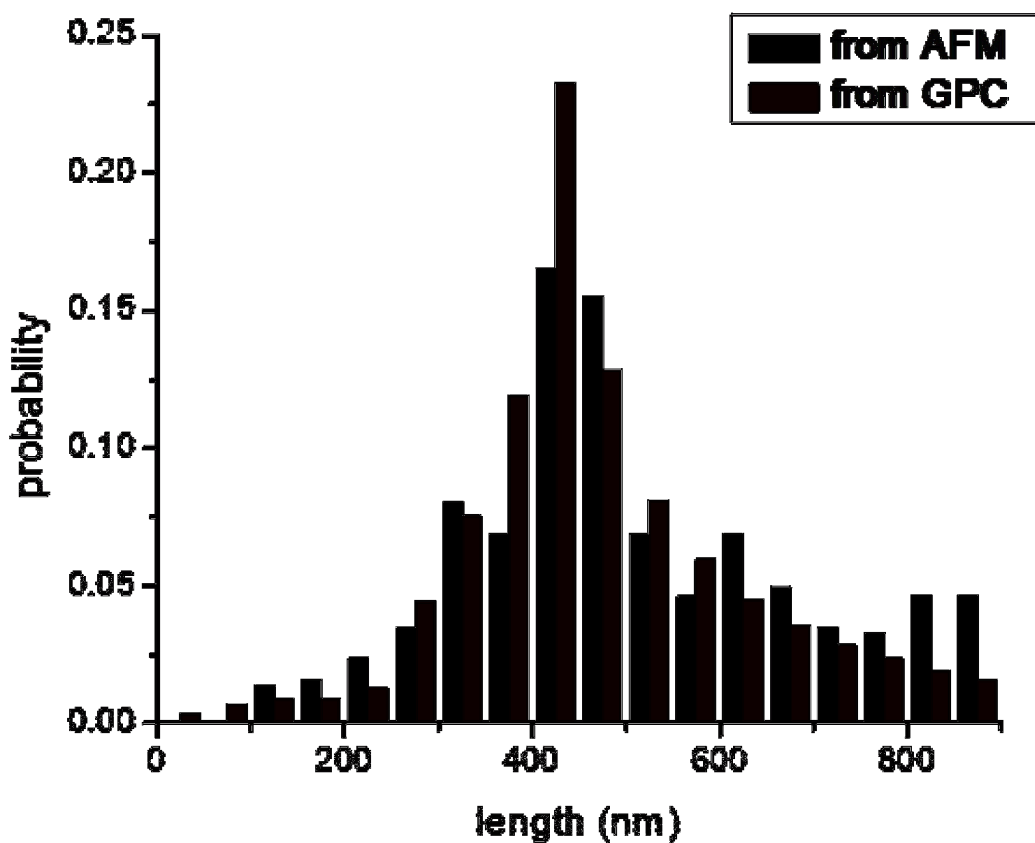


**Figure 9.** The distribution of contour length of PEOEMA analyte region of polymer **5b** derived from molecular weight distribution that was obtained from GPC (red) and the distribution of rupture length of polymer **5b** from AFM pulls (black). The length distributions are quite similar, indicating that the analyte is acting as the bridge between the AFM tip and the surface.

Interestingly, the independence of the contributions between polyelectrolyte and analyte regions allows the analyte to be characterized. The rupture length distribution of **5b** was compared to the contour length distribution of the analyte (PEOEMA) block derived from molecular weight distribution which was obtained from GPC-MALS (Figure 9). This analysis employs rupture length as a proxy for contour length. The two terms are not equivalent, but the relative stretch of a chain from 300 pN to 1000 pN is less than 10% (see, e.g. Figure 3). The majority of rupture forces fall within a much smaller range than this, with rupture forces that are close to typical model-

dependent values of contour length derived from extended freely jointed chain<sup>47</sup> or extended worm-like chain models.<sup>48</sup> The similar distributions indicate that during the pulling process, most of the polyelectrolyte block is wrapped on the tip and the elastically active subchain between the AFM tip and the surface is the analyte.

Another factor which could influence the magnitude of the electrostatic interaction is the solvent. When using water for the AFM pulling experiment, we did not obtain any rupture force higher than 200 pN, which is not surprising because hydration of the ions will dramatically decrease the interaction between the carboxylate (AFM tip) and the ammonium (polyelectrolyte handle). The strong interaction between water and ions is consistent with the high dielectric constant of water ( $\epsilon = 78.5$ ). When using DMF ( $\epsilon = 36.7$ ), the rupture force distribution increased significantly (Figure 10). It seemed that a decrease of the solvent dielectric constant and hydrogen bonding could lead to a stronger attraction between carboxylate and ammonium. However, when 1-butanol ( $\epsilon = 17.8$ ) and methyl benzoate ( $\epsilon = 7.5$ ) are used, the rupture force does not increase. In fact, the force distributions obtained in DMF, 1-butanol and methyl benzoate are quite similar (Figure 9). The similarity in rupture force distribution among these solvents implies that the association between carboxylate and ammonium does not change significantly. We note that the polymers **3a** and **3b** are readily dissolved in all three of these solvents after quaternization.

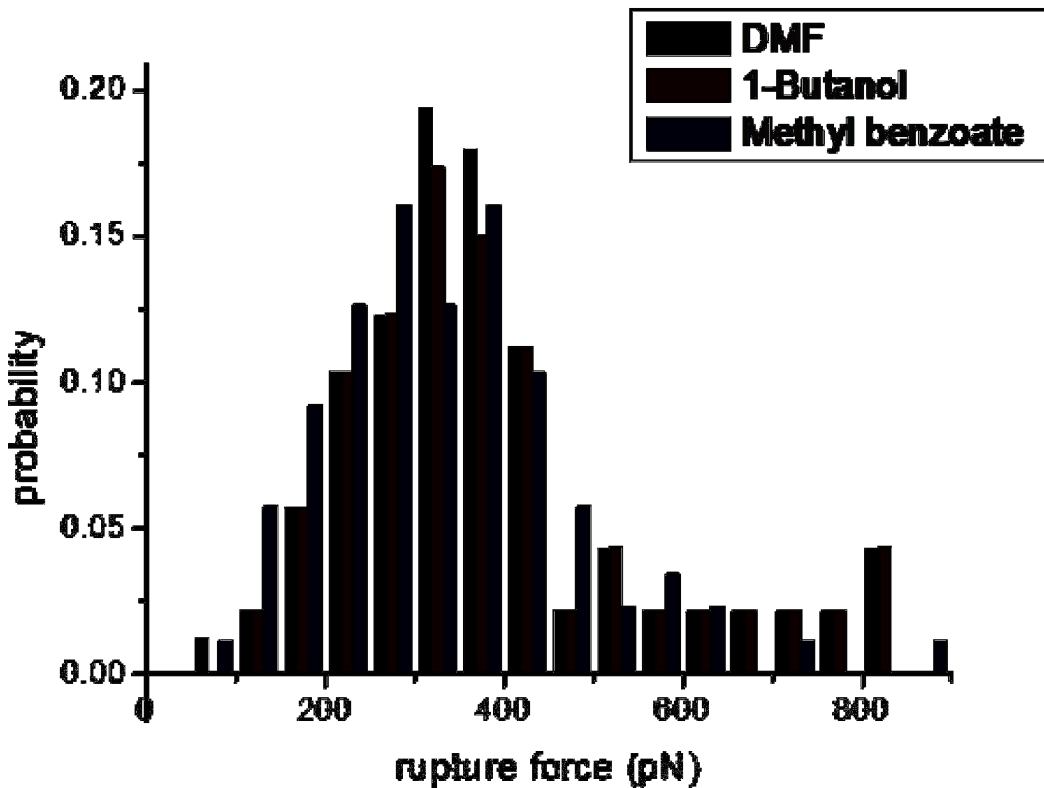


**Figure 10.** The rupture force distributions in DMF (black), 1-butanol (red) and methyl benzoate (blue). Carboxylate modified tip was used for the pulling experiment and the counterion of the polyelectrolyte is iodide. The most probable rupture forces of these three systems are quite close, ca. 330 pN.

To further test the influence of the solvent polarity, diphenyl ether ( $\epsilon = 3.9$ ) and mesitylene ( $\epsilon = 2.4$ ) were used for the experiments. No forces higher than 200 pN were obtained. This weak attachment is likely caused by the poor solubility of the polyelectrolyte in these solvents. During the AFM experiments, therefore, it is reasonable to expect that the PEOEMA block is well solvated whereas the quarternized PDMAEMA likely collapses and penetrates into the PEOEMA block to

minimize the contact with the solvents.<sup>35,49-50</sup> Such conformational rearrangement would reduce the availability of the PDMAEMA-tip interactions that drive rupture force.

To test the influence of counterions on the strength of the attachment, we used AgPF<sub>6</sub> to exchange the counterion from iodide to hexafluorophosphate. Figure 11 show that the average rupture force increased as the counterion changed from iodide into hexafluorophosphate. This trend is consistent with our assumption that using weakly coordinating counterion can decrease the “screening effect”<sup>40</sup> of the counterion on the polyelectrolyte and thus improve the association between the polyelectrolyte handle and the carboxylate modified tip. Unfortunately, simulations of the exact conformation of the handle on the tip and the nature of the dissociation process itself are sufficiently complex that we are not able to gain additional insights. Simulating “live” pulls is more difficult than simulating attachment conformation, because of the relatively long timescales of the experiments compared to the timescales in molecular simulations. Nonetheless, the simulations indicate (qualitatively) that dissociation is sensitive to the effective local dielectric constant at the AFM surface; see Supporting Information for details. It seems reasonable, although we are not able to test it here, that tip geometry would also have an impact.

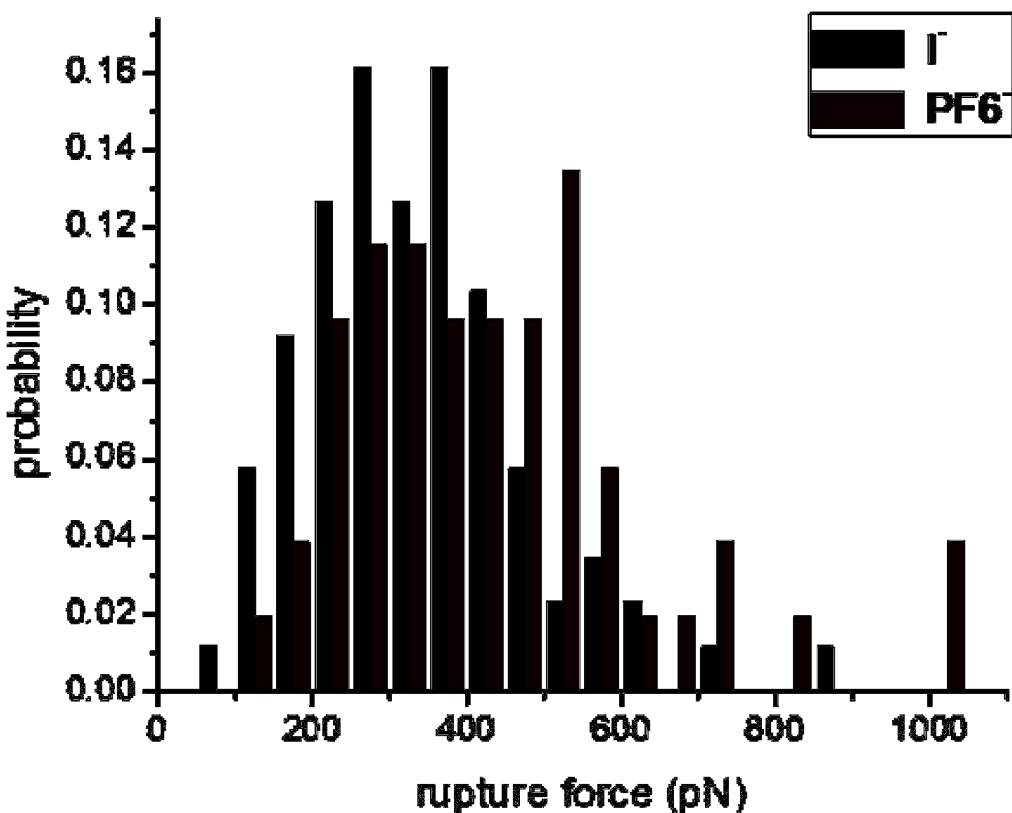


**Figure 11.** The rupture force distributions of polymer **5b** when iodide (black) and hexafluorophosphate (red) serve as counterions. Force distributions peak at ~300 pN in both cases. The AFM pulling experiments were conducted in methyl benzoate, and the carboxylate modified tip was used for pulling. When using hexafluorophosphate as counterion, the rupture force increased.

We also investigated the influence of the distance between the AFM tip and the surface when the AFM tip is waiting for the polymer to attach ( $L_0$ ) on the performance of the handle. A series of experiments were performed on polymer **5b** at different  $L_0$  when using the carboxylate modified AFM tips. Figure 12 shows the results of these experiments. As expected, it was found that when the waiting distance  $L_0$  increases, the probability of obtaining high rupture force decreases. Separations on the order of 10 nm can influence the interaction of the AFM tip and the polyelectrolyte dramatically. Here the radius of gyration of the polyelectrolyte is ca. 40 nm<sup>51</sup> and

the contour length is ca. 200 nm, suggesting that the radius of gyration is a more important length scale in affecting the interaction of the polyelectrolyte and the charged tip.

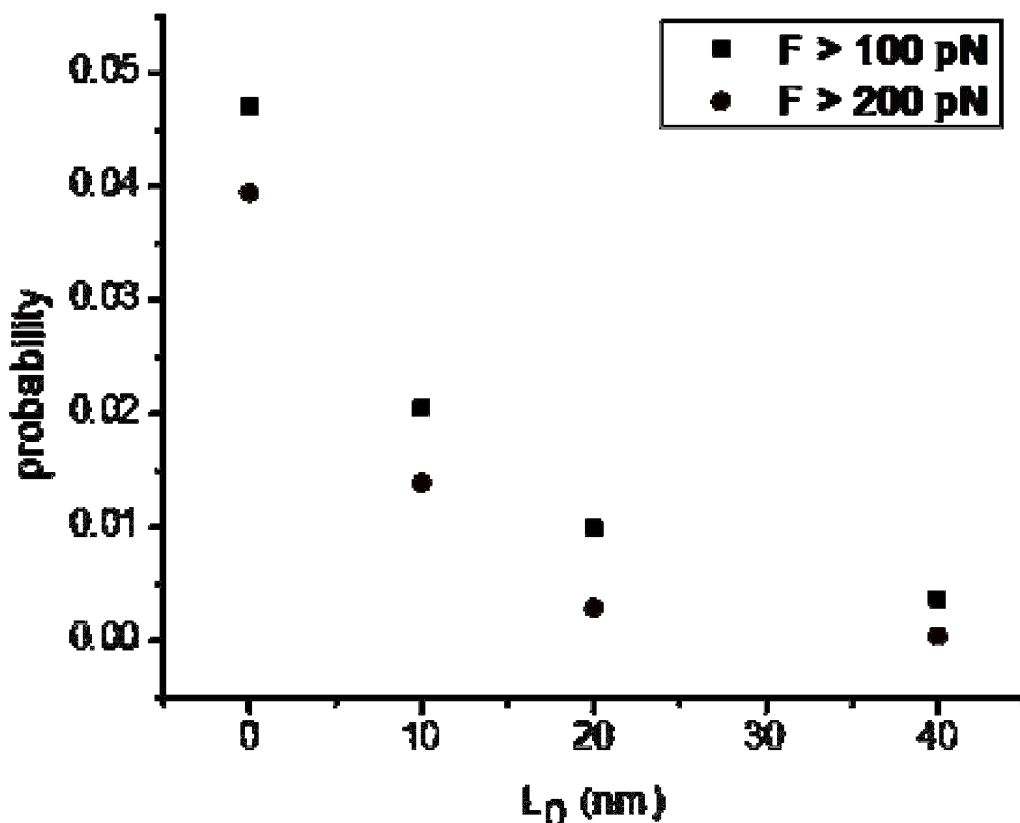


**Figure 12.** The probability of obtaining pulls in which rupture force higher than 100 pN (black) and higher than 200 pN (red) at different  $L_0$ .  $L_0$  is the distance between the AFM tip and surface when the AFM tip waits the polymer to attach. The experiments were conducted in methyl benzoate.

## Conclusion

We evaluate the utility of the polyelectrolyte handle strategy for single-molecule force spectroscopy “fishing” experiments<sup>52</sup> according to the four criteria we initially envisioned: 1) quick and efficient; 2) targeted; 3) strong; 4) reversibly detached. In the experiments reported here, the residence/waiting time for polymer-tip attachment was set to 5 seconds, which allows us to repeat

the approach/retract cycles thousands of times in a day. Under these conditions, the polyelectrolyte handle facilitated hundreds of successful pulls (with rupture forces of several hundred pN, such as the one shown in Figure 3), satisfying the efficient attachment criterion. Trends in both strength and length of bridging events with the size of the analyte and handle regions are consistent with an adsorption that is targeted to the handle with good specificity. Depending on the handle, the forces involved can be on the order of several hundred pN. Similar forces have been observed for nonspecific adsorption,<sup>53</sup> but here the adsorption is achieved without contact and with specific control of the position of attachment. The achieved force range is useful for some,<sup>15,21,30</sup> but certainly not all, substrates in covalent polymer mechanochemistry, our current area of interest. Regarding reversibility, polymer capture can be repeated multiple times with a single AFM tip, indicating that the ionic interaction is reversible under force. We therefore expect that the polyelectrolyte handle approach will prove useful for selected applications in covalent polymer mechanochemistry.

## ASSOCIATED CONTENT

**Supporting Information.** Simulation details; XPS characterization.

## AUTHOR INFORMATION

### Corresponding Author

\*To whom correspondence should be addressed. E-mail: stephen.craig@duke.edu

### Notes

The authors declare no competing financial interest.

## ACKNOWLEDGMENT

This material is based on work supported by the Center for Molecularly Optimized Networks, National Science Foundation, under grant CHE-2116298 and a Grant-In-Aid of Research from the National Academy of Sciences, administered by Sigma Xi, The Scientific Research Society (G20111015158063).

## REFERENCES

- (1) Binnig, G.; Quate, C. F.; Gerber, C. Atomic Force Microscope. *Phys. Rev. Lett.* **1986**, *56*, 930-933.
- (2) Florin, E. L.; Moy, V. T.; Gaub, H. E. Adhesion Forces between Individual Ligand-Receptor Pairs. *Science* **1994**, *264*, 415-417.
- (3) Janshoff, A.; Neitzert, M.; Oberdörfer, Y.; Fuchs, H. Force Spectroscopy of Molecular Systems—Single Molecule Spectroscopy of Polymers and Biomolecules. *Angew. Chem., Int. Ed.* **2000**, *39*, 3212-3237.
- (4) Hugel, T.; Seitz, M. The Study of Molecular Interactions by AFM Force Spectroscopy. *Macromol. Rapid Commun.* **2001**, *22*, 989-1016.
- (5) Zhang, X.; Liu, C.; Wang, Z. Force Spectroscopy of Polymers: Studying on Intramolecular and Intermolecular Interactions in Single Molecular Level. *Polymer* **2008**, *49*, 3353-3361.
- (6) Oberhauser, A. F.; Marszalek, P. E.; Erickson, H. P.; Fernandez, J. M. The Molecular Elasticity of the Extracellular Matrix Protein Tenascin. *Nature* **1998**, *393*, 181-185.
- (7) Zlatanova, J.; Lindsay, S. M.; Leuba, S. H. Single Molecule Force Spectroscopy in Biology Using the Atomic Force Microscope. *Prog. Biophys. Molec. Biol.* **2000**, *74*, 37-61.
- (8) Gunari, N.; Schmidt, M.; Janshoff, A. Persistence Length of Cylindrical Brush Molecules Measured by Atomic Force Microscopy. *Macromolecules* **2006**, *39*, 2219-2224.
- (9) Puchner, E. M.; Gaub, H. E. Force and Function: Probing Proteins with AFM-Based Force Spectroscopy. *Curr. Opin. Struct. Biol.* **2009**, *19*, 605-614.
- (10) Marszalek, P. E.; Dufrene, Y. F. Stretching Single Polysaccharides and Proteins Using Atomic Force Microscopy. *Chem. Soc. Rev.* **2012**, *41*, 3523-3534.
- (11) Bustamante, C.; Smith, S. B.; Liphardt, J.; Smith, D. Single-Molecule Studies of DNA Mechanics. *Curr. Opin. Struct. Biol.* **2000**, *10*, 279-285.
- (12) Wei, H.; van de Ven, T. G. M. AFM - Based Single Molecule Force Spectroscopy of Polymer Chains: Theoretical Models and Applications. *Appl. Spect. Rev.* **2008**, *43*, 111-133.
- (13) Sluysmans, D.; Lussis, P.; Fustin, C.-A.; Bertocco, A.; Leigh, D. A.; Duwez, A.-S. Real-Time Fluctuations in Single-Molecule Rotaxane Experiments Reveal an Intermediate Weak Binding State During Shuttling. *J. Am. Chem. Soc.* **2021**, *143*, 2348-2352.
- (14) Naranjo, T.; Lemishko, K. M.; de Lorenzo, S.; Somoza, A.; Ritort, F.; Pérez, E.; Ibarra, B. Dynamics of Individual Molecular Shuttles under Mechanical Force. *Nat. Commun.* **2018**, *9*, 4512.

(15) Beyer, M. K.; Clausen-Schaumann, H. Mechanochemistry: The Mechanical Activation of Covalent Bonds. *Chem. Rev.* **2005**, *105*, 2921-2948.

(16) Caruso, M. M.; Davis, D. A.; Shen, Q.; Odom, S. A.; Sottos, N. R.; White, S. R.; Moore, J. S. Mechanically-Induced Chemical Changes in Polymeric Materials. *Chem. Rev.* **2009**, *109*, 5755-5798.

(17) Ribas-Arino, J.; Marx, D. Covalent Mechanochemistry: Theoretical Concepts and Computational Tools with Applications to Molecular Nanomechanics. *Chem. Rev.* **2012**, *112*, 5412-5487.

(18) Kersey, F. R.; Yount, W. C.; Craig, S. L. Single-Molecule Force Spectroscopy of Bimolecular Reactions: System Homology in the Mechanical Activation of Ligand Substitution Reactions. *J. Am. Chem. Soc.* **2006**, *128*, 3886-3887.

(19) Wiita, A. P.; Ainavarapu, R. K.; Huang, H. H.; Fernandez, J. M. Force-Dependent Chemical Kinetics of Disulfide Bond Reduction Observed with Single-Molecule Techniques. *Proc. Natl. Acad. Sci. U. S. A.* **2006**, *103*, 7222-7227.

(20) Schmidt, S. W.; Beyer, M. K.; Clausen-Schaumann, H. Dynamic Strength of the Silicon–Carbon Bond Observed over Three Decades of Force-Loading Rates. *J. Am. Chem. Soc.* **2008**, *130*, 3664-3668.

(21) Liang, J.; Fernández, J. M. Mechanochemistry: One Bond at a Time. *ACS Nano* **2009**, *3*, 1628-1645.

(22) Wu, D.; Lenhardt, J. M.; Black, A. L.; Akhremitchev, B. B.; Craig, S. L. Molecular Stress Relief through a Force-Induced Irreversible Extension in Polymer Contour Length. *J. Am. Chem. Soc.* **2010**, *132*, 15936-15938.

(23) Klukovich, H. M.; Kouznetsova, T. B.; Kean, Z. S.; Lenhardt, J. M.; Craig, S. L. A Backbone Lever-Arm Effect Enhances Polymer Mechanochemistry. *Nat. Chem.* **2013**, *5*, 110-114.

(24) Wang, J.; Kouznetsova, T. B.; Niu, Z.; Ong, M. T.; Klukovich, H. M.; Rheingold, A. L.; Martinez, T. J.; Craig, S. L. Inducing and Quantifying Forbidden Reactivity with Single-Molecule Polymer Mechanochemistry. *Nat. Chem.* **2015**, *7*, 323-327.

(25) Sammon, M. S.; Biewend, M.; Michael, P.; Schirra, S.; Ončák, M.; Binder, W. H.; Beyer, M. K. Activation of a Copper Biscarbene Mechano-Catalyst Using Single-Molecule Force Spectroscopy Supported by Quantum Chemical Calculations. *Chem. Eur. J.* **2021**, *27*, 8723-8729.

(26) Pill, M. F.; East, A. L. L.; Marx, D.; Beyer, M. K.; Clausen-Schaumann, H. Mechanical Activation Drastically Accelerates Amide Bond Hydrolysis, Matching Enzyme Activity. *Angew. Chem., Int. Ed.* **2019**, *58*, 9787-9790.

(27) Zhang, H.; Li, X.; Lin, Y.; Gao, F.; Tang, Z.; Su, P.; Zhang, W.; Xu, Y.; Weng, W.; Boulatov, R. Multi-Modal Mechanophores Based on Cinnamate Dimers. *Nat. Commun.* **2017**, *8*, 1147.

(28) Wang, Z.; Kouznetsova, T. B.; Craig, S. L. Pulling Outward but Reacting Inward: Mechanically Induced Symmetry-Allowed Reactions of Cis- and Trans-Diester-Substituted Dichlorocyclopropanes. *Synlett* **2022**, *33*, 885-889.

(29) Kean, Z. S.; Craig, S. L. Mechanochemical Remodeling of Synthetic Polymers. *Polymer* **2012**, *53*, 1035-1048.

(30) Gossweiler, G. R.; Kouznetsova, T. B.; Craig, S. L. Force-Rate Characterization of Two Spiropyran-Based Molecular Force Probes. *J. Am. Chem. Soc.* **2015**, *137*, 6148-6151.

(31) Walder, R.; Van Patten, W. J.; Adhikari, A.; Perkins, T. T. Going Vertical to Improve the Accuracy of Atomic Force Microscopy Based Single-Molecule Force Spectroscopy. *ACS Nano* **2018**, *12*, 198-207.

(32) Ke, C.; Jiang, Y.; Rivera, M.; Clark, R. L.; Marszalek, P. E. Pulling Geometry-Induced Errors in Single Molecule Force Spectroscopy Measurements. *Biophysical Journal* **2007**, *92*, L76-L78.

(33) Rivera, M.; Lee, W.; Ke, C.; Marszalek, P. E.; Cole, D. G.; Clark, R. L. Minimizing Pulling Geometry Errors in Atomic Force Microscope Single Molecule Force Spectroscopy. *Biophysical Journal* **2008**, *95*, 3991-3998.

(34) Lowe, A. B.; McCormick, C. L. Synthesis and Solution Properties of Zwitterionic Polymers. *Chem. Rev.* **2002**, *102*, 4177-4190.

(35) Granville, A. M.; Boyes, S. G.; Akgun, B.; Foster, M. D.; Brittain, W. J. Synthesis and Characterization of Stimuli-Responsive Semifluorinated Polymer Brushes Prepared by Atom Transfer Radical Polymerization. *Macromolecules* **2004**, *37*, 2790-2796.

(36) Lokaj, J.; Vlček, P.; Kříž, J. Synthesis of Polystyrene-Poly(2-(Dimethylamino)Ethyl Methacrylate) Block Copolymers by Stable Free-Radical Polymerization. *Macromolecules* **1997**, *30*, 7644-7646.

(37) Zhang, X.; Xia, J.; Matyjaszewski, K. Controlled/“Living” Radical Polymerization of 2-(Dimethylamino)Ethyl Methacrylate. *Macromolecules* **1998**, *31*, 5167-5169.

(38) Zhang, X.; Matyjaszewski, K. Synthesis of Well-Defined Amphiphilic Block Copolymers with 2-(Dimethylamino)Ethyl Methacrylate by Controlled Radical Polymerization. *Macromolecules* **1999**, *32*, 1763-1766.

(39) Zeng, F.; Shen, Y.; Zhu, S.; Pelton, R. Atom Transfer Radical Polymerization of 2-(Dimethylamino)Ethyl Methacrylate in Aqueous Media. *J. Polym. Sci. A: Polym. Chem.* **2000**, *38*, 3821-3827.

(40) Duwez, A.-S.; Guillet, P.; Colard, C.; Gohy, J.-F.; Fustin, C.-A. Dithioesters and Trithiocarbonates as Anchoring Groups for the “Grafting-to” Approach. *Macromolecules* **2006**, *39*, 2729-2731.

(41) Serpe, M. J.; Rivera, M.; Kersey, F. R.; Clark, R. L.; Craig, S. L. Time and Distance Dependence of Reversible Polymer Bridging Followed by Single-Molecule Force Spectroscopy. *Langmuir* **2008**, *24*, 4738-4742.

(42) Florin, E. L.; Rief, M.; Lehmann, H.; Ludwig, M.; Dormair, C.; Moy, V. T.; Gaub, H. E. Sensing Specific Molecular-Interactions with the Atomic-Force Microscope. *Biosens Bioelectron* **1995**, *10*, 895-901.

(43) Wu, T.; Gong, P.; Szleifer, I.; Vlcek, P.; Subr, V.; Genzer, J. Behavior of Surface-Anchored Poly(Acrylic Acid) Brushes with Grafting Density Gradients on Solid Substrates: 1. Experiment. *Macromolecules* **2007**, *40*, 8756-8764.

(44) Brandrup, J.; Immergut, E. H.; Grulke, E. A. *Polymer Handbook*. **1999**, Wiley: New York.

(45) Good, R. J. Contact-Angle, Wetting, and Adhesion - a Critical-Review. *J. Adh. Sci. Tech.* **1992**, *6*, 1269-1302.

(46) Azzaroni, O.; Brown, A. A.; Huck, W. T. S. Tunable Wettability by Clicking Counterions into Polyelectrolyte Brushes. *Adv. Mater.* **2007**, *19*, 151-154.

(47) Smith, S. B.; Cui, Y.; Bustamante, C. Overstretching B-DNA: The Elastic Response of Individual Double-Stranded and Single-Stranded DNA Molecules. *Science* **1996**, *271*, 795-799.

(48) Petrosyan, R. Improved Approximations for Some Polymer Extension Models. *Rheologica Acta* **2017**, *56*, 21-26.

(49) Rowe, M. D.; Hammer, B. A. G.; Boyes, S. G. Synthesis of Surface-Initiated Stimuli-Responsive Diblock Copolymer Brushes Utilizing a Combination of Atrp and Raft Polymerization Techniques. *Macromolecules* **2008**, *41*, 4147-4157.

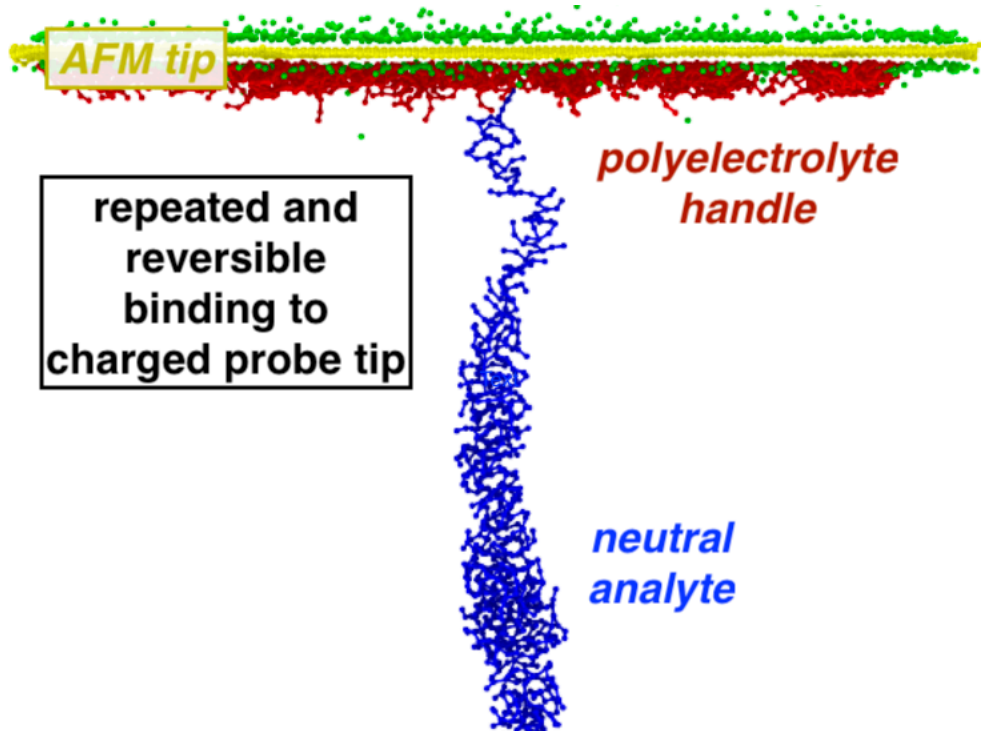
(50) Barbey, R.; Lavanant, L.; Paripovic, D.; Schuewer, N.; Sugnaux, C.; Tugulu, S.; Klok, H.-A. Polymer Brushes Via Surface-Initiated Controlled Radical Polymerization: Synthesis, Characterization, Properties, and Applications. *Chem. Rev.* **2009**, *109*, 5437-5527.

(51) Nierlich, M.; Boue, F.; Lapp, A.; Oberthur, R. Radius of Gyration of a Polyion in Salt Free Poly-Electrolyte Solutions Measured by Sans. *J. Physique* **1985**, *46*, 649-655.

(52) Struckmeier, J.; Wahl, R.; Leuschner, M.; Nunes, J.; Janovjak, H.; Geisler, U.; Hofmann, G.; Jaehnke, T.; Mueller, D. J. Fully Automated Single-Molecule Force Spectroscopy for Screening Applications. *Nanotechnology* **2008**, *19*, 384020.

(53) Zhang, B.; Shi, R.; Duan, W.; Luo, Z.; Lu, Z.-y.; Cui, S. Direct Comparison between Chemisorption and Physisorption: A Study of Poly(Ethylene Glycol) by Means of Single-Molecule Force Spectroscopy. *RSC Advances* **2017**, *7*, 33883-33889.

Insert Table of Contents Graphic and Synopsis Here



A polyelectrolyte block provides reversible and repeatable binding to the tip of atomic force microscope that allows the force-extension behavior of a neutral analyte block to be characterized.